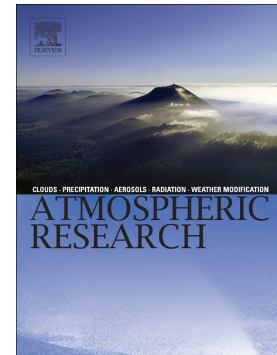


## Journal Pre-proof

Assimilation of radar radial velocity data with the WRF hybrid 4DEnVar system for the prediction of hurricane Ike (2008)

Feifei Shen, Dongmei Xu, Jinzhong Min, Zhigang Chu, Xin Li



PII: S0169-8095(19)30463-6

DOI: <https://doi.org/10.1016/j.atmosres.2019.104771>

Reference: ATMOS 104771

To appear in: *Atmospheric Research*

Received date: 16 April 2019

Revised date: 24 September 2019

Accepted date: 18 November 2019

Please cite this article as: F. Shen, D. Xu, J. Min, et al., Assimilation of radar radial velocity data with the WRF hybrid 4DEnVar system for the prediction of hurricane Ike (2008), *Atmospheric Research*(2018), <https://doi.org/10.1016/j.atmosres.2019.104771>

This is a PDF file of an article that has undergone enhancements after acceptance, such as the addition of a cover page and metadata, and formatting for readability, but it is not yet the definitive version of record. This version will undergo additional copyediting, typesetting and review before it is published in its final form, but we are providing this version to give early visibility of the article. Please note that, during the production process, errors may be discovered which could affect the content, and all legal disclaimers that apply to the journal pertain.

© 2018 Published by Elsevier.

## Assimilation of Radar Radial Velocity Data with the WRF Hybrid 4DEnVar System for the Prediction of Hurricane Ike (2008)

Feifei Shen<sup>1</sup>, Dongmei Xu<sup>1,\*</sup> xdmjolly@sina.com, Jinzhong Min<sup>1</sup>, Zhigang Chu<sup>1</sup>, and Xin Li<sup>2</sup>

<sup>1</sup>Key Laboratory of Meteorological Disaster, Ministry of Education (KLME)/Joint International Research Laboratory of Climate and Environment Change (ILCEC)/Collaborative Innovation Center on Forecast and Evaluation of Meteorological Disasters (CIC-FEMD), Nanjing University of Information Science & Technology, Nanjing 210044, China

<sup>2</sup>Key Laboratory of Transportation Meteorology, CMA, and Jiangsu Research Institute of Meteorological Sciences, and Nanjing Joint Center of Atmospheric Research, Nanjing, China

\*Corresponding author.

### Abstract

Four dimensional ensemble-variation data assimilation (4DEnVar) is the method that considers the flow dependent background error covariance (BEC) and asynchronous observations throughout the assimilation window, which avoids the maintenance of the adjoint model. The impacts of assimilation of radial velocity (Vr) data using hybrid-4DEnVar for the analyses and forecasts of hurricane Ike are investigated using Weather Research and Forecasting and Data Assimilation model (WRFDA). 4DEnVar is coupled with Ensemble Transform Kalman Filter (ETKF) by updating the ensemble mean by the hybrid scheme and the ensemble perturbations are updated by the ETKF. Single observation tests for typical Jet cast and tropical cyclone (TC) case are conducted before the real hurricane Ike (2008) case. It is found that the analysis increment moves downstream by the end of the assimilation window. The linear propagation represented by the 4DEnVar method is close to the full nonlinear model integration. For the real IKE case, it is found that positive and spiral temperature increments, best track and intensity forecast are found in 4DEnVar experiment, indicating a more realistic thermal structure of hurricane Ike. 3DEnVar and 3DVar-FGAT are limited due to the lack of the BEC description spatially and temporally. 3DVar experiment produces much smoother and weaker increments with cold temperature increments at the hurricane vortex center at lower levels.

Keywords: radial velocity data; WRF data assimilation; 4DEnVar; numerical simulation

## 1. Introduction

Basic variational data assimilation (DA) refers to three-dimensional (3DVar) or a four-dimensional (4DVar) approach to provide optimized initial conditions in numerical weather prediction (NWP) model. Variational DA methods are widely used

in operational NWP centers as well as research centers (Sun et al., 2016). 4DVar is more sophisticated compared to 3DVar, which involves three spatial and one temporal dimensions. 4DVar aims to find the trajectory that best fits the past and present observations to estimate the flow-dependent error referred as background error covariance (BEC) matrix, but it generally requires iteration of an adjoint model. Thus, the computational cost of 4DVar and the effort to develop and maintain the adjoint model is rather demanding. BEC is an important component in data assimilation system, largely dominating the error correlations between different analysis variables. BEC allows DA to determine the weight to more accurate data (observation or background) and also to spread observational information between different model variables. To take advantage of the flow-dependent and time dependent error covariances from the ensemble based DA method, hybrid variational/ensemble approaches are proposed by Hamill and Snyder (2000) to express the BEC as a linear combination of static and ensemble based contributions in the variational cost function. The hybrid approaches are on the increase with the consideration of limited ensemble size due to restricted supercomputing capacity (Pan et al., 2014).

New data assimilation methods are highly required to utilize the strengths of each data assimilation method while reducing their individual weaknesses. Four dimensional ensemble-variational data assimilation (4DEnVar) is the method that considers the flow dependent BEC and time dependent observations. It computes the evolving uncertainty directly from the ensemble, replacing the linear approximation used in 4DVar, thus avoiding the maintenance of the adjoint model. 4DEnVar system needs to be coupled with another independent ensemble DA system to update the ensemble members, such as the Ensemble Kalman Filter (EnKF; Evensen, 1994) and Ensemble Transform Kalman Filter (ETKF; Bishop et al., 2001).

Early studies on such coupled data assimilation method for 4DEnVar include proposing, testing, and demonstrating new algorithms using simple models and simulated observations (e.g., Qiu et al., 2007; Tian et al., 2008; Liu et al., 2008; Liu et al., 2009; Wang et al., 2010; Desroziers et al., 2014; Fairbairn et al., 2014). More recently, the 4DEnVar method has been implemented and successfully investigated

for global NWP models (Andrew, et al., 2014, Buehner et al., 2010a,b; Buehner 2013; Kleist and Ide 2015a,b; Lorenc et al., 2015). In Liu et al., (2009), a localized matrix is introduced into the algorithm for ensemble covariance localization and Liu and Xiao (2013) further applied it to real data problems. Buehner et al., (2010b) performed an intercomparison study for the Canadian operational global NWP model, and found that the 4DEnVar improved upon their operational, nonhybrid-4DVar in the tropics and Southern Hemisphere, but not in the Northern Hemisphere. It was also found that 4DEnVar performed slightly worse than a hybrid-4DVar. Buehner et al., (2013) further compared 4DEnVar, 3DVar, and 4DVar for global weather prediction. They found that 4DEnVar is always better than 3DVar and is either similar or better than 4DVar in the tropical troposphere and the winter extratropical regions. Wang and Lei (2014) performed a comparison study of hybrid 4DEnVar with the three dimensional ensemble-variational data assimilation (3DEnVar) using the NCEP GFS (model) at a low resolution. They found that 4DEnVar is better than 3DEnVar, with a larger impact in the extratropical atmosphere than in the tropics. Kleist and Ide (2015b) evaluated hybrid-4DEnVar with various initialization techniques within the National Centers for Environmental Prediction Global Data Assimilation System (GDAS) using simulated data. They found that the hybrid-4DEnVar can reduce analysis error for most variables at most levels, especially in the extratropics, compared to hybrid 3DEnVar. Finally, Lorenc et al., (2015) compared hybrid-4DVar and hybrid-4DEnVar. Hybrid-4DVar was found to perform better than hybrid-4DEnVar in the Met Office global operational system. It is noted that the 4DEnVar algorithm is a natural extension of earlier proposed 3DEnVar (Lorenc 2003; Buehner 2005; Wang et al., 2007, 2008a, 2008b; Wang 2010). Lu et al., (2017) found using 4DEnVar to assimilate tail Doppler radar (TDR) data improves the analyzed storm intensity forecasts compared to 3DEnVar although 4DEnVar slightly degrades the track forecast.

In addition, 4DEnVar is expected to be extremely suitable for four-dimensional observations with high spatial or/and temporal resolution, such as radar observation. Wang et al., (2013a) improved short-term quantitative precipitation forecasting (QPF)

using a 4DVar technique in Weather Research and Forecasting Model (WRF). Li et al., (2012) and Shen et al., (2016) used 3DEnVar in the framework of WRF to assimilate radial velocity ( $V_r$ ) data for the prediction of hurricanes. Most of these studies fully or partially apply a three dimensional (3DVar, 3DEnVar) or four dimensional (4DVar, En4DVar) variational method (Wang et al., 2013a, 2013b).

Despite the successful applications of the various 4D ensemble-variational approaches, to date there is no published study applying a hybrid-4DEnVar method to the assimilation of radar data at a convection-allowing resolution for tropical cyclone (TC) predictions. In the current study, the authors apply a hybrid-4DEnVar system for the WRF model to examine the effectiveness of a 4D ensemble data assimilation system that does not require linearized models. Results are compared with a 3DVar, 3DVar-First Guess at Appropriate Time (FGAT, Rabier et al., 1998, Lawless 2010), and the 3DEnVar method in the TC analysis and forecast respectively. Meanwhile, this study also investigates the impact of the linear assumption for the temporal propagation through covariance of ensemble perturbations. The rest of the manuscript is organized as follows. In Section 2 we briefly describe the hybrid-3DEnVar and hybrid-4DEnVar DA schemes. A set of single-observation experiments are conducted to diagnose the behavior of the 4D ensemble covariance in Section 3; We present the configuration of the experiments and the analysis and forecast results from each experiment in Section 4 and 5. A summary and some further discussion are provided in Section 6.

## 2 Methodology

### 2.1 WRF hybrid-3DEnVar system

The variational method is typically a non-probabilistic approach to provide a single estimate of the state optimally. Given a first guess of the state (background) with the covariance matrix  $B$ , and the observation with the covariance matrix  $R$ , the updated state minimizes the departure to both the background and the observation with a cost

function. Practically, the algorithm is realized with the incremental as the control variable. Details can be referred in WRFDA (Wang et al., 2008a,b, Barker et al., 2012). At  $t=0$ , the cost function is composed of the background term  $J_b$  and the observation term  $J_o$ , which is formed as,

$$\begin{aligned} J(\mathbf{x}') &= J_b(\mathbf{x}') + J_o(\mathbf{x}') \\ &= \frac{1}{2} \mathbf{x}'^T \mathbf{B}^{-1} \mathbf{x}' + \frac{1}{2} (\mathbf{H}\mathbf{x}' - \mathbf{d})^T \mathbf{R}^{-1} (\mathbf{H}\mathbf{x}' - \mathbf{d}) \end{aligned} \quad (1)$$

where  $\mathbf{x}'$  is the analysis increment,  $\mathbf{H}$  is the linearized observation operator of the full observation operator  $\mathbf{H}$ .  $\mathbf{d} = \mathbf{y} - \mathbf{H}(\mathbf{x}_0^b)$  is the innovation by using the full nonlinear observation operator  $\mathbf{H}$ .  $\mathbf{y}$  is the observation and  $\mathbf{x}_0^b$  is the background. The cost function is modified to include the flow-dependent BEC by extending the control variables  $\mathbf{a}$  as,

$$\begin{aligned} J(\mathbf{x}_1', \mathbf{a}) &= \beta_1 J_b + \beta_2 J_e + J_o \\ &= \beta_1 \frac{1}{2} \mathbf{x}_1'^T \mathbf{B}^{-1} \mathbf{x}_1' + \beta_2 \frac{1}{2} (\mathbf{a})^T \mathbf{A}^{-1} (\mathbf{a}) + \frac{1}{2} (\mathbf{d} - \mathbf{H}\mathbf{x}')^T \mathbf{R}^{-1} (\mathbf{d} - \mathbf{H}\mathbf{x}') \end{aligned} \quad (2)$$

Here,  $\mathbf{x}_1'$  is the increment associated with the static BEC and  $\mathbf{x}'$  is the total increment of hybrid. The sum of  $J_b$  and  $J_e$  with each weight  $\beta_1$  and  $\beta_2$  replaces the traditional 3DVar background term  $J_b$ .  $J_e$  is associated with the ensemble based BEC.  $\mathbf{A}$  performs localization of the ensemble BEC by controlling the spatial correlation of extra control variable  $\mathbf{a}$ , which contains  $\mathbf{a}_k$  ( $k = 1, \dots, K$ ) for the  $K$  ensemble member. The hybrid-3DEnVar analysis increment is formed with the static  $\mathbf{x}_1'$  and flow-dependent BEC  $\sum_{k=1}^K (\mathbf{a}_k \circ \mathbf{x}_k^e)$  respectively, as,

$$\mathbf{x}' = \mathbf{x}_1' + \sum_{k=1}^K (\mathbf{a}_k \circ \mathbf{x}_k^e) \quad (3)$$

, where  $\mathbf{x}_k^e$  ( $k=1, \dots, K$ ) is the  $k$ th ensemble perturbations normalized by  $\sqrt{K-1}$  (Wang 2010).

## 2.2 WRF hybrid-4DVar system

To expand the time dimension from  $t=0$  to  $t=\tau$ , the cost function of hybrid-4DVar (ensemble BEC incorporated with 4DVar) is,

$$\begin{aligned} J(\mathbf{x}'_1, \mathbf{a}) &= \beta_1 J_b(\mathbf{x}'_1) + \beta_2 J_e(\mathbf{a}) + J_o(\mathbf{x}'_1, \mathbf{a}) \\ &= \beta_1 \frac{1}{2} \mathbf{x}'_1{}^T \mathbf{B}^{-1} \mathbf{x}'_1 + \beta_2 \frac{1}{2} \mathbf{a}^T \mathbf{A}^{-1} \mathbf{a} \quad , \quad (4) \\ &\quad + \frac{1}{2} \sum_{t=0}^{\tau} (\mathbf{H}_t \mathbf{x}'_k - \mathbf{d}_t)^T \mathbf{R}_t^{-1} (\mathbf{H}_t \mathbf{x}'_k - \mathbf{d}_t) \\ &\quad \mathbf{x}'_k = \mathbf{M}_t \mathbf{x}'_1 \quad , \quad (5) \end{aligned}$$

where  $\mathbf{d}_t$  is the innovation from different times as,  $\mathbf{d}_t = \mathbf{y}_t - \mathbf{H}_t [\mathbf{M}_t(\mathbf{x}'_1)]$ .  $\mathbf{M}_t$  is tangent linear version of the full integration model  $\mathbf{M}_t$ .  $\mathbf{H}_t$  is the linearized observation operator at different times. The analysis increments  $\mathbf{x}'_1$  represents for the analysis increment at the beginning of the time window from the static BEC. Similar with hybrid-3DVar, the final hybrid-4DVar analysis increment is formed with the static  $\mathbf{x}'_1$  and  $\sum_{k=1}^K (\mathbf{a}_k \circ \mathbf{x}'_k)$  with the flow-dependent BEC.

It is found that in hybrid-4DVar equals to hybrid-3DVar when  $\tau=0$ , the tangent linear model  $\mathbf{M}$  and its adjoint  $\mathbf{M}^T$  have to be employed in hybrid-4DVar minimization. The total analysis increment in observation spaces is formed as

$$\mathbf{H}_t \mathbf{M}_t \mathbf{x}' = \mathbf{H}_t \mathbf{M}_t \mathbf{x}'_1 + \mathbf{H}_t \frac{1}{\sqrt{K-1}} \sum_{k=1}^K (\mathbf{a}_k \circ \mathbf{M}_t \mathbf{x}'_k) \quad . \quad (6)$$

Eq. 6 can be further changed to avoid the linear approximation in the forward model,

$$\mathbf{H}_t \mathbf{M}_t \mathbf{x}' \approx \mathbf{H}_t \mathbf{x}'_1 + \mathbf{H}_t \frac{1}{\sqrt{K-1}} \sum_{k=1}^K \left\{ \mathbf{a}_k \circ \left[ \mathbf{M}_t(\mathbf{x}'_k) - \overline{\mathbf{M}_t(\mathbf{x}'_k)} \right] \right\} \quad , \quad (7)$$

$\mathbf{M}_t$  is neglected in the first term and second terms. The propagation of the ensemble perturbation is replaced by the perturbation of the nonlinear ensemble forecast, where  $\overline{\mathbf{M}_t(\mathbf{x}^e)}$  is the ensemble forecast mean at time  $t$ . The analysis increment is actually a linear combination of the predicted ensemble perturbations. The assumption in the first term and second terms in Eq. (7) is equivalent to that in 3DVar-FGAT (Vialard et al., 2003, Weaver et al., 2003, Barret et al., 2008) and 4DEnVar (Schwartz et al., 2015, Liu et al., 2009, Liu et al., 2008b) respectively (Poterjoy and Zhang 2016). The ensemble members are updated together with the ETKF method (Bishop et al., 2001), which uses an transform matrix without localization. Here  $\mathbf{M}_t$  is linearized about a nonlinear forecast from the beginning of the assimilation window to time  $t$  with  $\mathbf{M}_t(\mathbf{x}^e)$ , with a simplified physical parameterization schemes.

### 3. Single-observation experiments

Several single observation experiments that assimilate only one single pseudo observation are performed to diagnose the behavior of the 4D ensemble covariances within the WRF hybrid-4DEnVar framework. We choose two different cases. A strong midlatitude jet stream case and a hurricane case are applied to represent the situation for strong advection and complex nonlinear physics as well as moist processes respectively.

The WRF model (Skamarock et al., 2008) is employed as the forecast model, which is a three-dimensional, compressible, non-hydrostatic atmospheric model. The physical parameterizations are used as follows: the WRF Single-Moment 6-Class scheme (Hong et al., 2004); the Yonsei University (YSU) boundary layer scheme (Noh et al., 2003; Hu et al., 2013); the 5-layer thermal diffusion model for land surface processes scheme; the Rapid Radiative Transfer Model (RRTM) longwave radiation scheme (Mlawer et al., 1997); and the MM5 shortwave radiation scheme

(Dudhia, 1989); the Grell-Devenyi cumulus parameterization (Grell and Devenyi, 2002). The case-dependent static BEC matrixes are estimated with the National Meteorological Center (NMC) method (Parrish and Derber, 1992) based on the differences of the 24 and 12 h forecasts initiated from Global Forecast System (GFS) analyses at 0000 and 1200 UTC for each day for a month. The two pseudo-observations are described in Table 1.

Table 1. The two observation types for the single-observation experiments in section 3

Case	Jet stream	Hurricane Ike
Direction	Westerly	Southerly
$y - y^0$	10 m/s	10 m/s
Location	41°N, 41°W (500 hPa)	28.6°N, 92.6°W (850 hPa)
Time	0300 UTC 1 Nov 2011	0300 UTC 13 Sep 2008

### 3.1 Single-observation tests for Jet case.

For the first case, the polar jet stream is located in the region of North Atlantic Ocean in the southeast of Newfoundland. The model domain is configured with  $150 \times 150$  grids horizontally and 41 levels vertically with 30 km resolution. The observation is described in the Table 1. A westerly wind is located at (41°N, 41°W) with an innovation of 10 m/s at a pressure of about 500 hPa. The wind speed for this example is about 60 m/s. Forecast ranges of 3-h, 6-h, and 9-h are initialized from 0000 UTC 1 November 2011. Fig. 1 shows the jet stream wind fields for the background  $\mathbf{x}^b$  at 0300 UTC, 0600 UTC (the analysis time), and 0900 UTC 1 November 2011, which is treated as fg01 (the 1st first guess), fg02 (2nd first guess), and fg03 (the 3rd first guess) respectively. The assimilation window is defined between these times. The observation is located at the beginning of the assimilation window at the time of 0300 UTC, referred as ob01 (the first observation). In addition, the observation is chosen to reside upstream from the base of a shortwave trough, similar to the single-observation experiments shown in Buehner et al. (2010a).

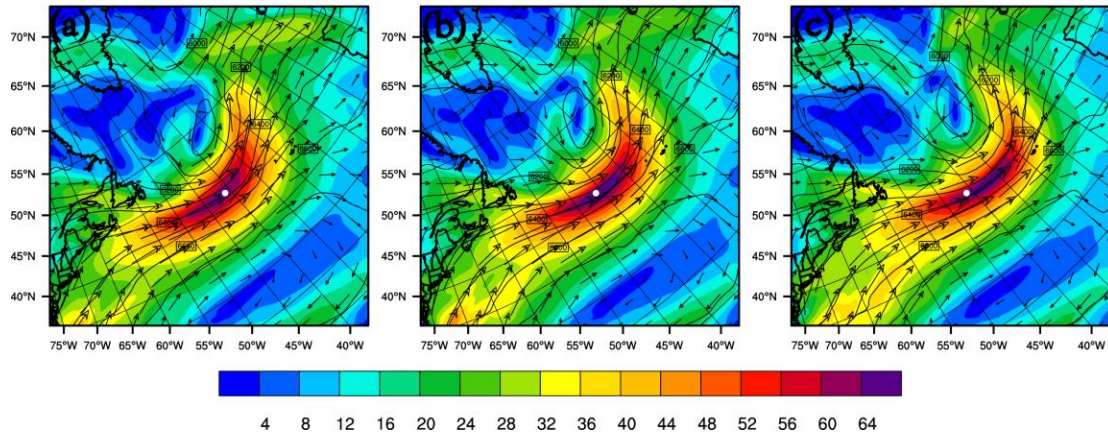


FIG. 1. Plot of the background wind fields for the jet stream example at 500 hPa, at times (a) 0300 (b) 0600 and (c) 0900 UTC 1 Nov 2011 (shaded, wind magnitude (m/s), Solid line, the pressure contours). The observation is located at the white dot, but is only present at 0300 UTC.

For the Jet case, we conduct three single-observation tests to investigate the sensitivity of the WRF hybrid-4DEnVar to ensemble size over the 6-h assimilation window. All of the single-observation experiments used a 500 km horizontal localization length scale and 100% ensemble covariance. The single-observation experiments with 20, 40 and 80 members (refer to as 4DEnVar-20m, 4DEnVar-40m, 4DEnVar-80m, respectively). The same single-observation test can be utilized to further investigate the impact of temporal evolution of the flow dependent ensemble BEC in 4DEnVar, by differentiating the analysis increments at various times. For the 4DEnVar algorithm, the propagation of information is achieved implicitly through correlations represented by the 4D ensemble perturbations with a limited ensemble size. In 4DEnVar-20m, a single wind observation at 0300 UTC 1 November 2011 was assimilated. It is evident that the analysis increment at the beginning of the window (Fig. 2a) exhibits a heterogeneous structure, since the ensemble covariance captures the “errors of the day.” In addition, the center of the maximum increment was more closely collocated with the location of the observation. Also note that the analysis increment in 4DEnVar-20m experiment that utilized 100% ensemble BEC covariances exhibits a wind increment that is stretched along the height gradient as would be expected. Fig. 2d shows the resulting analysis increment of wind at 500 hPa valid at the middle of the 6-h assimilation window. Relative to the observation location (black dot), the center of

the maximum increment was displaced downstream toward the east and northeast during the 6-h assimilation window. This result was consistent with that the analysis time was 3-h later than the observation time and the prevailing background wind was blowing eastward. The increments have moved downstream by the end of the assimilation window (Fig. 2g). Given the severity of the sampling error with only 20 ensemble members (Fig. 2a, d, g), we performed two additional sensitivity experiments denoted 4DEnVar-40m and 4DEnVar-80m. The ensemble size is increased from 20 to 40 members in 4DEnVar-40m, leading to relatively smaller sampling errors (Fig. 2b, e, h). We further increase the ensemble size of the 4DEnVar experiment to 80 members (4DEnVar-80m) to compare with the other two sensitivity experiments. A larger ensemble size improves the estimate of the flow dependent ensemble BEC and therefore reduce the sampling errors to a level, again suggesting that would result in a more reliable estimate of the ensemble BEC, followed by appropriate analysis increments. Overall, All the three sensitivity experiments show the temporal evolution of the observation information, though the observation is set only at the beginning of the assimilation window (Fig. 2a, b, c). It is expected that 4DEnVar experiment with more ensemble members is able to better capture the error of the day, indicating Fig. 2c, f, i in the right column is most appropriate analysis increment.

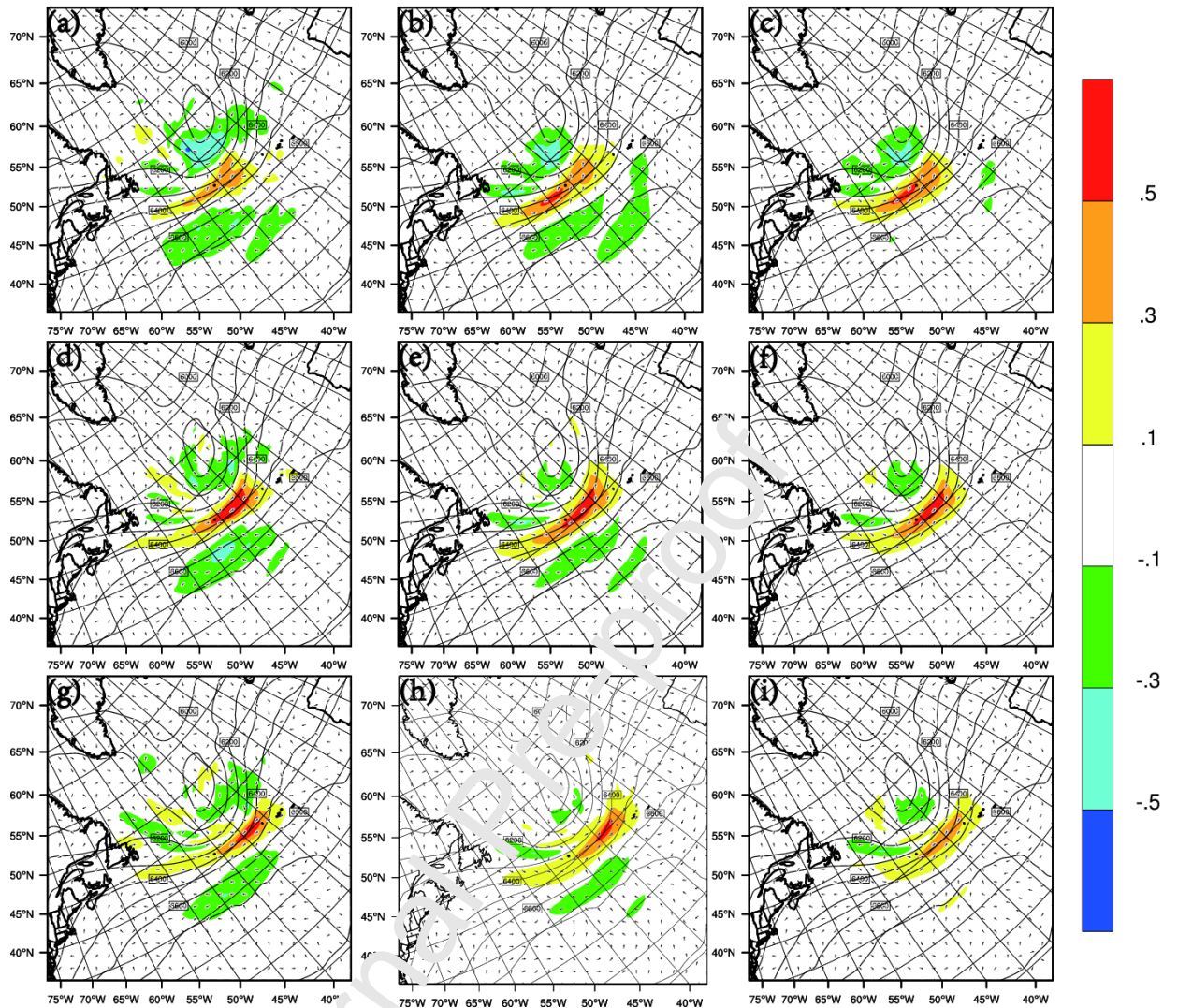


FIG. 2. 500-hPa wind analysis increment (unit, m/s) valid at the beginning (1st row), middle (2nd row), and end (3rd row) of the assimilation window for the 4DEnVar-20m (first column), 4DEnVar-40m (second column) and 4DEnVar-80m (third column). The black solid contours are the background 500-hPa geopotential height (dam) valid at the center (middle) of the assimilation window.

The single-observation experiments are further designed to explore the 4D representation of the climatological and ensemble BECs for hybrid-4DEnVar. Four single-observation experiments (Conv model i, ii, iii, iv in Table 2) are further designed with different weights of ensemble background error covariance (EBE) and static background error covariance (SBE) to illustrate the effect of 4D ensemble

covariance. They are also designed to explore the effect of horizontal localization (listed in table 2) on the ensemble covariance. The single observations are located at the beginning of the assimilation window. The analysis increments are plotted for the background times (i. e., -3h, 0, +3h) to illustrate the impact of the temporal evolution of the ensemble BEC in the hybrid-4DEnVar.

Table 2. Covariance (Cov) models used for the single-observation experiments.

Cov model	i	ii	iii	iv
SBE	1.0	0.0	0.0	0.5
EBE	0.0	1.0	1.0	0.5
L (km)	-	500	1200	1200

Firstly, the hybrid-4DEnVar analysis increments with 100% ensemble BEC in Cov model ii are compared for Cov model i, where the pure static climatological covariance is employed. The increments from Cov model i and Cov model ii are shown in Figs. 3a–c and Figs. 3d–f respectively. For Cov model i, hybrid-4DEnVar is equivalent to 3DVar-FGAT. A homogeneous structure is observed at the start of the assimilation window (Fig. 3a) with the use of the 3D climatological covariance. For the following 6-h assimilation window (middle and end), the analysis increments look very similar with the increment in the beginning during the assimilation window. (Fig. 3b, c) with no temporal evolution.

Cov model ii uses a pure ensemble covariance in hybrid-4DEnVar with a 500 km localization scales. It is noted that there is a heterogenous structure in the analysis increment at the beginning of the window of 0300 UTC 13 September (Fig. 3d), with the “errors of the day” captured by the ensemble covariance. The analysis increment moves downstream by the end of the assimilation window at 0600 UTC 13 September.

Cov model iii is the same as Cov model ii but applies relatively relaxed localization length scale of 1200 km. The analysis increments are expected to spread out over a larger area. It seems that the wind increments from the Cov model iii suffers from spurious correlations in terms of sampling error more so than that from the Cov model ii which applies a shorter localization scale. The spurious correlations are identified using the reference of the increments in Figs 2c, 2f, 2i with a rather larger ensemble size. It indicates that in this case, given an ensemble with 80 or more members, broader localization is still suitable.

Cov model iv is same with cov model iii, but with mixed hybrid background-error covariance matrix. The analysis increments for Cov model iv are expected to be a linear combination of the increments for Cov model i and Cov model iii effectively. It should be noted that the spurious correlation problem is reduced by adding a time-invariant, static contribution to the background error covariance clearly, whereas it still maintains the 4D nature of the increment (Kleist. et al. 2015).

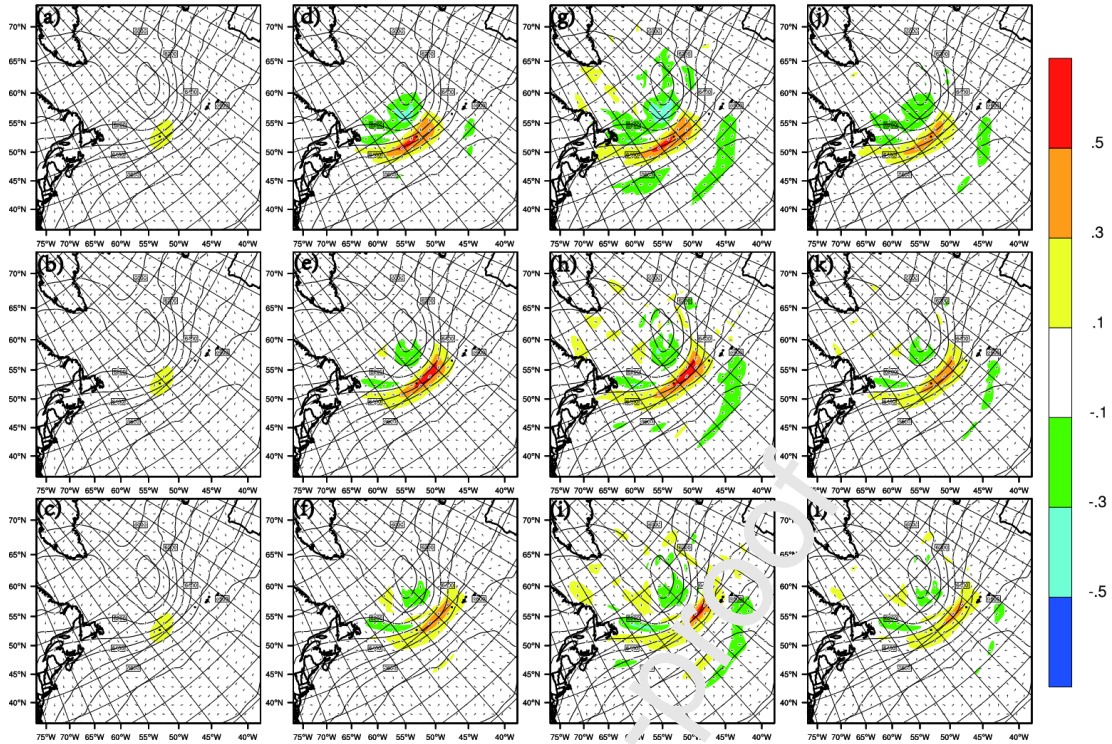


FIG. 3. Wind analysis increments for the hurricane case. Using Cov model i: (a) hybrid-4DVar increment at the start of the window, (b) at the middle of the window, and (c) at the end of the window. (d)–(f), (g)–(i), (j)–(l) Equivalent to (a)–(c) and correspond to Cov models ii, iii, and iv, respectively. As in Fig. 2 the dot shows the observation position.

### 3.2 Single-observation tests for Hurricane case.

For the Hurricane case, the model domain has a  $515 \times 515$  horizontal grid and 43 vertical levels up to 30 hPa model top and the grid spacing is 4 km. Hurricane Ike is chosen as the second case, which is one of the strongest hurricanes in 2008, with its eye located near southern Cuba. Fig. 4 shows the wind fields of fg01 at 0300 UTC, fg02 at 0600 UTC, and fg03 at 0900 UTC at 850 hPa on 13 September 2008. The strongest winds are observed in the eastern of its eye. The observation is designed in the east of the hurricane of the location (28.6°N, 92.6°W, 850 hPa) at 0300 UTC at 13

Sep 2008 only for the beginning of assimilation window in Table 1. Only a 40 ensemble members are applied instead of 80 ensemble members in the jet case, due to the computational reasons for the configuration with a rather high resolution (5 km with  $401 \times 401 \times 41$  model grids) for hurricane Ike. The relatively small ensemble size is not likely to change the conclusions of the experiments, since it still keeps the ability of the hybrid-4DEnVar to propagate the increment through the assimilation window.

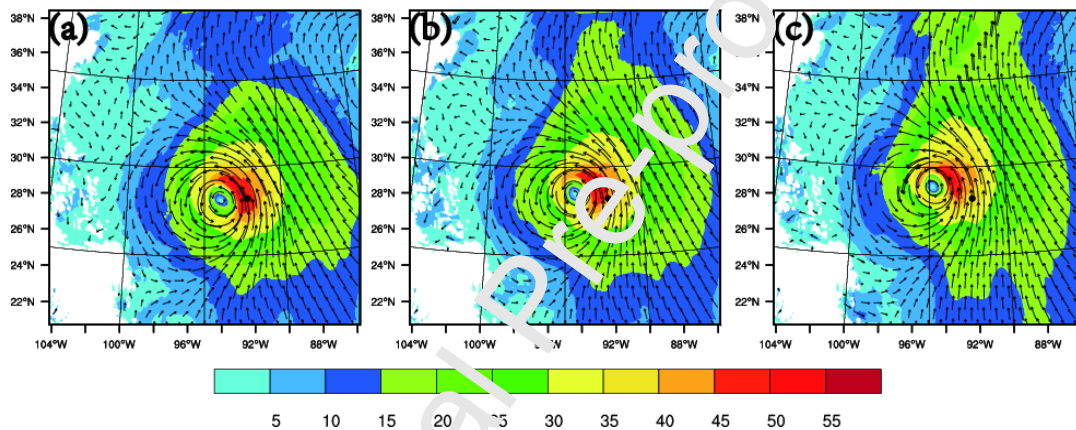


FIG. 4. Background wind fields for the hurricane Ike at 850 hPa, at times (a) 0300 (b) 0600 and (c) 0900 UTC 1 September 2008 (shaded, wind magnitude (m/s)).

Cov model i, ii, iii, iv in Table 2 are also applied to the hurricane case to illustrate the effect of ensemble BEC and different horizontal localization on the analysis increment with relatively higher resolution. The geopotential height analysis increments are shown for different assimilation window times (i. e., -3 h, 0 h, +3 h) with the single observation located at the beginning of the assimilation window. Similarly with the jet case, the increments from Cov model i with the pure static climatological covariance, a notable dipole structure is observed during the whole data assimilation window (Fig. 5a-c) with no temporal evolution. The increments of

the geopotential height suggested the assimilation of the single wind observation at  $t = -3\text{h}$  corrected the position of the hurricane in the background forecast at  $t = 0$  by moving the vortex with low geopotential height northward, which is consistent with Wang and Lei (2014). By using a pure ensemble covariance in hybrid-4DEnVar in Cov model with a 500 km localization scales. A heterogenous pattern in the analysis increment at the beginning of the window of 0300 UTC 13 September (Fig. 5d) is observed with the flow-dependent BEC from the ensembles. When increasing the localization length scale from 500 km to 1200 km, the analysis increments spread over a larger area (for example in the northeast side of the domain), which may introduce spurious correlations especially for the hurricane case with smaller scales compared to the jet case, by comparing the 2nd column and the 3rd column in Fig. 5. Cov model iv applies a mixed hybrid background-error covariance matrix, which alleviates the spurious correlation problem and keeps the 4D nature of the increment by partly introducing a time-invariant, static background error covariance.

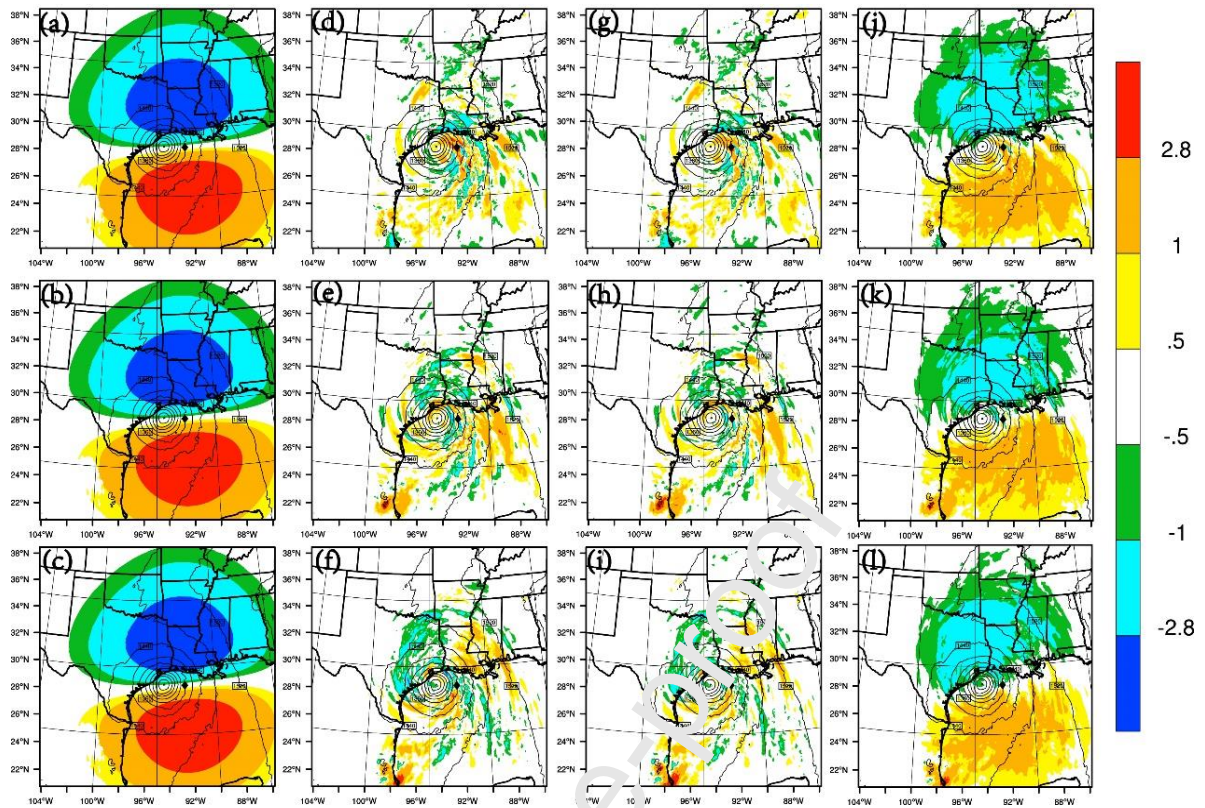


Fig. 5. Same as Fig.3 but for the geopotential height increments (color shades, units: m) at 850 hPa for the hurricane case.

In 4DEnVar, the temporal propagation of observation information within the data assimilation window is effectively achieved through covariance of ensemble perturbations at discrete times. Although the ensemble forecasts were generated by full nonlinear model integrations, the temporal propagation through covariance of ensemble perturbations contains a linear assumption. Several single observation tests are conducted to illustrate how well the nonlinear propagation is implicitly represented by the 4DEnVar method when compared to the full nonlinear model integration. First, the single wind observation in Table 1 at  $t=-3$  h was assimilated with the 3DVar method to generate the analysis valid at  $t=-3$  at 0300 UTC 13 September 2008. Two forecasts were launched by the states at  $t=-3$  h with and without

assimilating the single observation, respectively. The difference in the two forecasts are shown in Fig. 6a, reflecting the increment valid at  $t = 0$  by propagating the increment at  $t = -3$  h using the full nonlinear model integration. Therefore, it can be served as the verification reference of increments generated by 4DEnVar and 3DEnVar. The spatial pattern of the geopotential height increment (Fig. 6a) contains small-scale information and a dipole structure close to the center with a negative and a positive increment in the north and the south of the hurricane inner core area respectively. Similar to Fig. 5, the dipole structure is related to the vortex movement after DA. The increments from 4DEnVar in Figs 6b, 6c, and 6d using 100%, 80%, 75% ensemble BECs perform rather similarly and stably in two aspects. Firstly, the increments from Fig. 6b-6d are positive and negative in the south and north of the hurricane center. Secondary, small-scale inhomogeneous increments from Fig. 6b-6d are found to approximate those from the nonlinear model in Fig. 6a with similar spiral patterns. When further decreasing the ensemble weight to 25%, 0%, the increment with a clear and dominant dipole structure is observed in Figs. 6e and 6f. The negative and the positive increments on the north and the south side of the eyes become stronger due to the use of the 100% static BEC generated from NMC method. When the single observation located at  $t=0$  is assimilated with 3DEnVar, the increment becomes smaller in both magnitude and scale. Such increment is probably due to the use of the 100% ensemble based BEC, which is likely to include smaller background error than those in the static BEC. In Fig. 6h, the isotropy static background covariance contribute to 100% weight leading to a large increment with a strong

homogenous pattern.

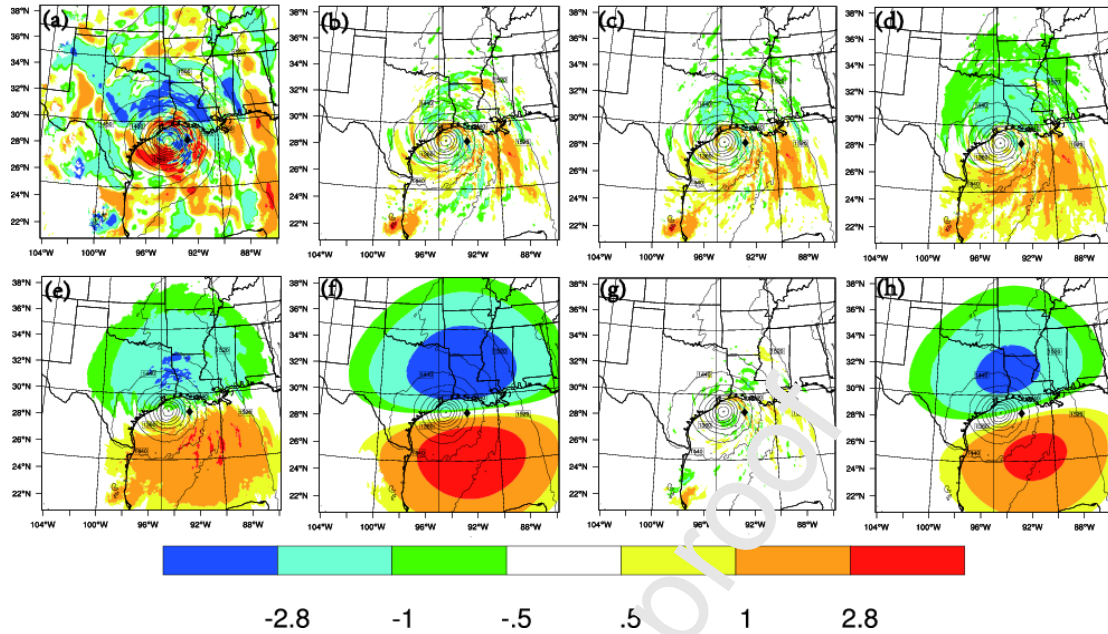


FIG. 6. Geopotential height increments (color shades, units: m) at 850 hPa valid at the middle of a 6-h assimilation window after assimilating a single meridional wind observation. Black contours are background height fields valid at the middle of the assimilation window. The observation was located at the black square sign and valid at the beginning of the assimilation window. Increments are by (a) model integration, 4D-EnVar with (b) 100% ensemble weight, (c) 75% ensemble weight, (d) 50% ensemble weight, (e) 25% ensemble weight, (f) 0% ensemble weight, (g) 3D-EnVar with 100% ensemble weight, and (h) 3D-EnVar with 0% ensemble weight

From the single observation tests, it is found that larger ensemble size is able to better capture the error of the day. For both jet case and hurricane case, there are heterogeneous structures in the analysis increment at the beginning of the assimilation window, with the “errors of the day” captured by the ensemble covariance, which can be transformed to the end of the assimilation window. Also note that the linear propagation represented by the 4D-EnVar method is close to the full nonlinear model integration.

## 4. Real observation experiments

### 4.1 The model configuration

The WRF model (Skamarock et al., 2008) is employed as the forecast model,

which is a three-dimensional, compressible, non-hydrostatic atmospheric model. The model domain has a  $515 \times 515$  horizontal grid and 43 vertical levels up to 30 hPa model top and the grid spacing is 4 km. The physical parameterizations are used as follows: the WRF Single-Moment 6-Class scheme (Hong et al., 2004); the Yonsei University (YSU) boundary layer scheme (Noh et al., 2003; Hu et al., 2013); the 5-layer thermal diffusion model for land surface processes scheme; the Rapid Radiative Transfer Model (RRTM) longwave radiation scheme (Mlawer et al., 1997); and the MM5 shortwave radiation scheme (Dudhia, 1989); the Grell-Devenyi cumulus parameterization (Grell and Devenyi, 2002).

## 4.2 The data assimilation setup

To better illustrate the features of the WRF hybrid-4DVar, four data assimilation experiments denoted as 3DVar, 3DVar-FGAT, 3DVar, and 4DVar are conducted. Table 3 summarizes the experimental configurations. All experiments assimilated radar Vr data since it is found in previous study (Shen et al., 2015), that the background state without Vr data assimilation is too coarse to enhance the inner-core structure. 3DVar is provided as a benchmark for comparison, which ignores the flow-dependent background error and the temporal evolution of the BEC. 3DVar-FGAT applied multiple time slots, but treating all the innovation valid at the center without including the ensemble-based BEC. The BEC estimated from the ensemble valid at the center of the assimilation window is used in 3DVar, while 4DVar considers the time evolution of the BEC by spanning the assimilation

window. The case is based on the hurricane Ike, which is one of the strongest hurricanes in 2008 in Atlantic.

Table 3

Experiment Name	Time Slot	Ensemble Perturbation(EP)
1 3DVar	1	N/A
2 3DVar-FGAT	3	N/A
3 3DEnVar	1	EP02(center)
4 4DEnVar	3	EP01(-15min), EP02(center), EP03(+15min)

The data assimilation starts from 0000 UTC on 12 September 2008 to 0300 UTC on 13 September 2008 every 30 minutes for 3DVar, 3DVar-FGAT, 3DEnVar and 4DEnVar. In 3DVar and 3DVar-FGAT, the background is the forecast initiated 6-h earlier from the NCEP operational GFS  $0.5^\circ \times 0.5^\circ$  analysis at 1800 UTC on 12 September 2008. For 3DEnVar and 4DEnVar, 40 ensemble forecasts were generated by randomly perturbing the GFS analysis valid at 1800 UTC 12 September 2008. Except for the experiment with 40 ensemble members, we also conducted experiments that used 20 and 60 ensemble members respectively. It is found that the analysis increments, the resulting track, and intensity forecasts of the experiment with 20 ensemble size is noticeably inferior to those of 40 or 60 ensembles, similar to the finding of Li et al. [2012]. It is also found that experiments with 60 members yield results rather comparable or slightly better than experiments with 40 members. Due to the demanding cost with large ensemble size and the limited computational resource, this study focuses on the comparison of the results with 40 ensemble members. Ensemble members are initially dynamically balanced using the CV5 BEC statistics

in the WRFDA system. The ensemble forecast means are applied as the first guesses in 3DVar and 4DVar. Radar Vr observations within  $\pm 5$  min of each analysis time in 3DVar and 3DVar are assimilated setting the observation error 2 m/s empirically. The quality control of the Vr observations is conducted using the 88d2arps package in the ARPS model and the SOLO software (Oye et al., 1995) developed by NCAR to identify unwanted radar echoes. The details of the radar observations and quality control can be found in Shen et al. (2017) for reference. For 3DVar-FGAT and 4DVar, observations and corresponding backgrounds at three time slots (-15 min, 0 min, +15 min) are prepared for calculating the innovations. 3DVar and 4DVar evolve one group and 3 groups of ensemble perturbations respectively with 60 km and 3 km for zonal and vertical localization scales. 18-h deterministic forecasts are conducted for all the experiments either initialized from the deterministic analysis or the ensemble analyses mean.

## 5. Results

### 5.1 ensemble forecasts

The key component of the WRF hybrid-4DVar is incorporating the temporal evolution of the error covariance within the assimilation window in a flow dependent manner. The ensemble spread of wind and temperature for the three assimilation windows (-15 min, 0, +15 min) at the 18th model level (close to 500 hPa) is shown in Fig. 7 valid at 2345 UTC 12 September 0000 UTC 13 September and 0015 UTC 13 September respectively. The ensemble spread reveals patterns that reflect observation

locations as well as features of the weather conditions (Shen et al., 2015). Large spread is found in the center of hurricane Ike for temperature and winds, reflecting larger forecast uncertainty of hurricane Ike. It is found that the patterns and the magnitude of the spreads vary with the forecast leading time, indicating the error of the day. The temporal evolution of the flow-dependent error is expected to be utilized in the 4DEnVar.

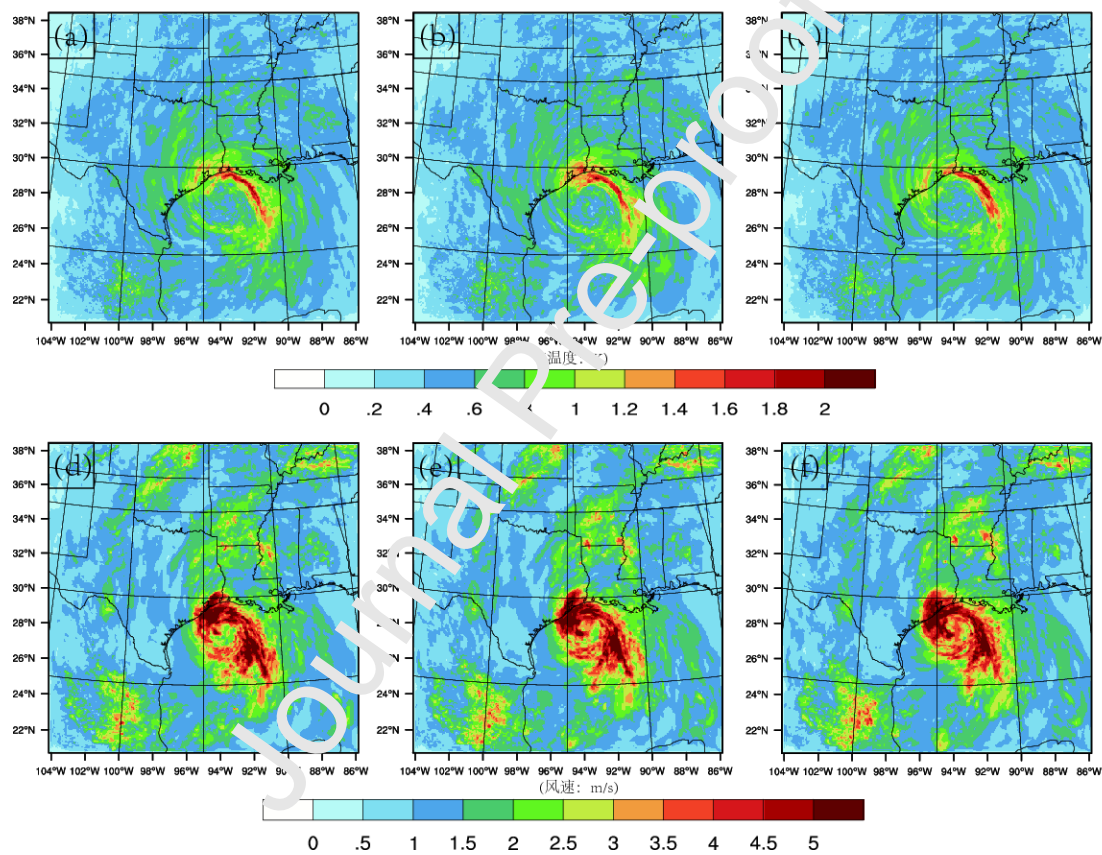


FIG. 7. Ensemble spread for (a-c) temperature (K), (d-f) wind speed (m/s) valid at (a,d) 2345 UTC 12, (b,e) 0000UTC 13, (c,f) 0015UTC 13 September 2008 at the 9 th model level

## 5.2 Verification for the analyses

Fig. 8 show the analysis increments of temperature at 850 hPa from all experiments at 0000 UTC on September 13 2008. It is noted that there is a negative

temperature increment in 3DVar, which is consistent with the results in previous studies (Shen et al., 2016). It indicates that warm core of the hurricane Ike is weakened with the assimilation of Radar Vr data from 3DVar based on a climatological static background error. The increment in 3DVar-FGAT is similar with 3DVar, since the algorithm in 3DVar-FGAT approximates 3DVar in terms of the static BEC. The difference consists in 3DVar-FGAT and 3DVar is that the former applies innovations from multiple times and treats all the innovations valid at the analysis time. As a benefit of the flow-dependent multivariate covariance, spiral temperature increment patterns with positive temperature increments are yielded by both 3DVar and 4DVar exist at the center of hurricane Ike, especially for the first DA cycle, which indicates the formation of the warm core structure for hurricane Ike. It seems that there are larger temperature increments in 4DVar than that in 3DVar as a benefit of the temporal evolution and multi-variable cross-correlations represented by ensemble perturbations.

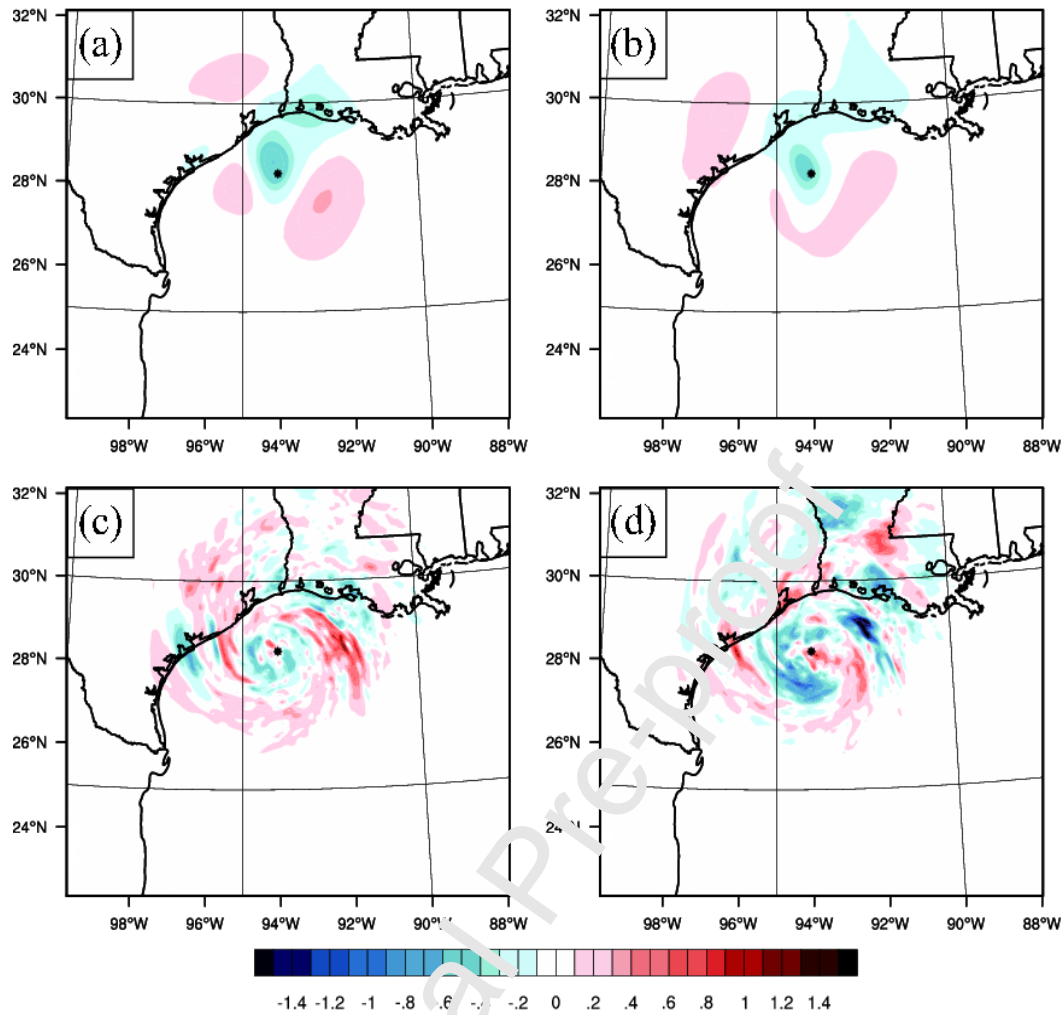


Fig. 8. Temperature analysis increments (shaded contours, unit: K) at 850 hPa for (a)3DVar (b) 3DVar-FGAT (c) 3DEnVar (d) 4DEnVar at 0000 UTC on September 13, 2008.

Fig. 9 shows the sea level pressure and wind at 0000 UTC on September 13 2008 for the four DA experiments. It is obvious that the TC structures in 3DVar and 3DVar-FGAT are relatively weak with minimum sea level pressure (MSLP) close to 955 hPa and 954 hPa compared to the best track data of 951 hPa in National Hurricane Center (NHC) even after assimilating the radar Vr observation. The MSLP in 3DEnVar and 4DEnVar are 952 hPa and 951 hPa relatively, fitting the best track more closely due to the inclusion of the error of the day from the ensembles. The TC structures are better adjusted with the appropriate BEC from 3DEnVar and 4DEnVar.

The largest improvement in 4D<sub>En</sub>Var is likely reflecting the contribution from the spatially inhomogeneous and temporal evolution of the flow-dependent ensemble BEC in terms of balancing the wind and pressure fields.

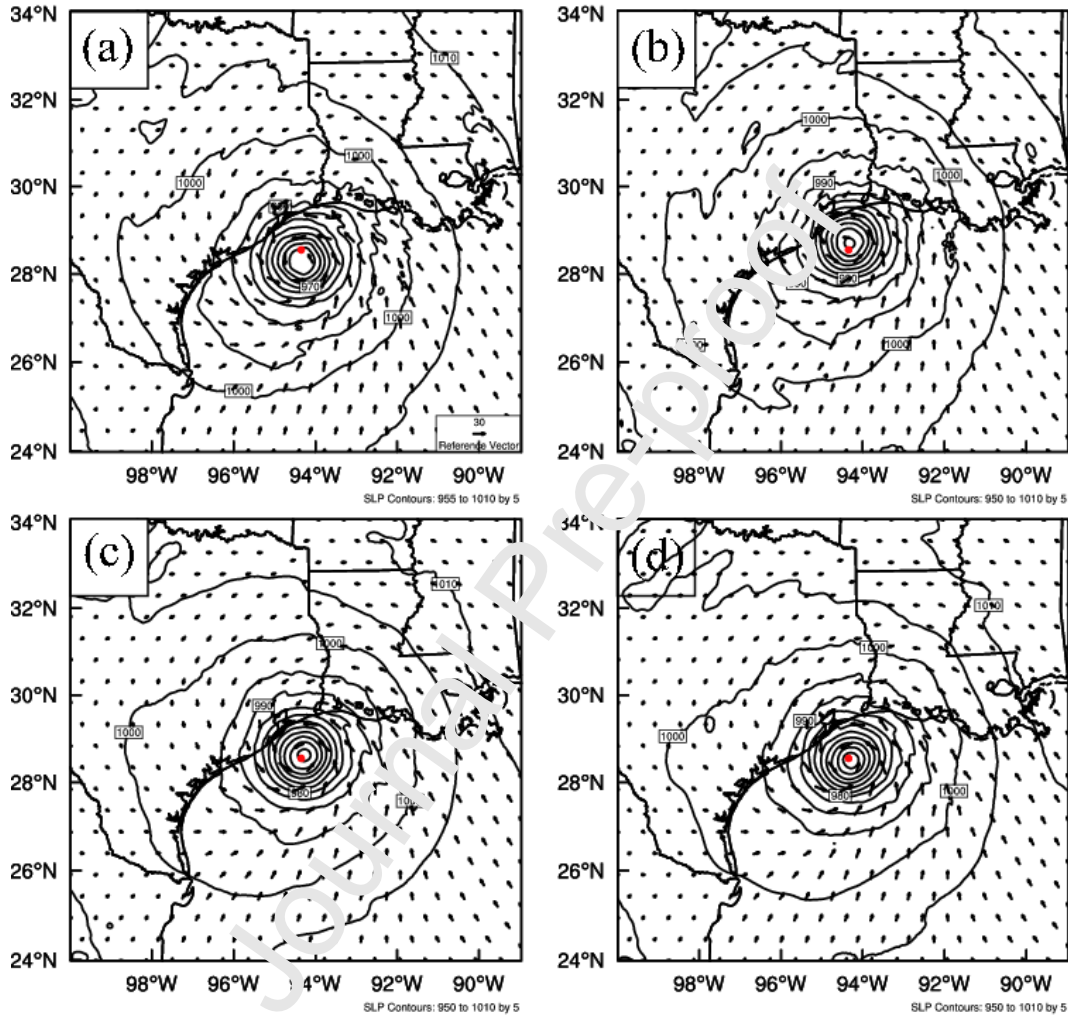


Fig. 9. Sea level pressure and wind for (a)3D<sub>Var</sub> (b) 3D<sub>Var</sub>-FGAT (c) 3D<sub>En</sub><sub>Var</sub> (d) 4D<sub>En</sub><sub>Var</sub> at 0300 UTC on September 13, 2008. (The red dots indicate the approximate center location of the observed TC).

To evaluate how well the forecasts and analyses model state fit the  $V_r$  observations, the diagnostic statistics of the root-mean-square error (RMSE) are quantitatively presented in Fig. 10 (Dowell et al. 2004; Yussouf et al. 2013). The RMSEs are calculated based on the simulated  $V_r$  with the analyzed ensemble mean

using the observation operator against the  $V_r$  observation from the Houston, Texas WSR-88D (KHGX) and the Lake Charles, Louisiana WSR-88D (KLCH) during the DA cyclings. The RMSE reduced 7.3 m/s, 7.3 m/s, 5.1 m/s and 6 m/s for 3DEnVar, 4DEnVar, 3DVar, and 3DVar-FGAT in the first DA cycle most significantly compared with other cycles. Generally, RMSEs increase roughly 1–2 m/s with 30 min forecasts after DA as expected. In the final analysis, the RMSEs of 3DEnVar and 4DEnVar are around 3.39 m/s and 3.2 m/s while for 3DVar and 3DVar-FGAT, the final RMSEs are 4.5 m/s and 4.05 m/s respectively. Generally, 4DEnVar yields smallest RMSEs, while largest RMSE occurs for 3DVar. It seems that 3DEnVar always fit better to the observations than that of 4DEnVar with an error growth less than 4DEnVar, suggesting that 3DEnVar analyses are more balanced than that of 4DEnVar. This is probably due to the use of observations with multiple time slots in 4DEnVar, which needs more time to be balanced.

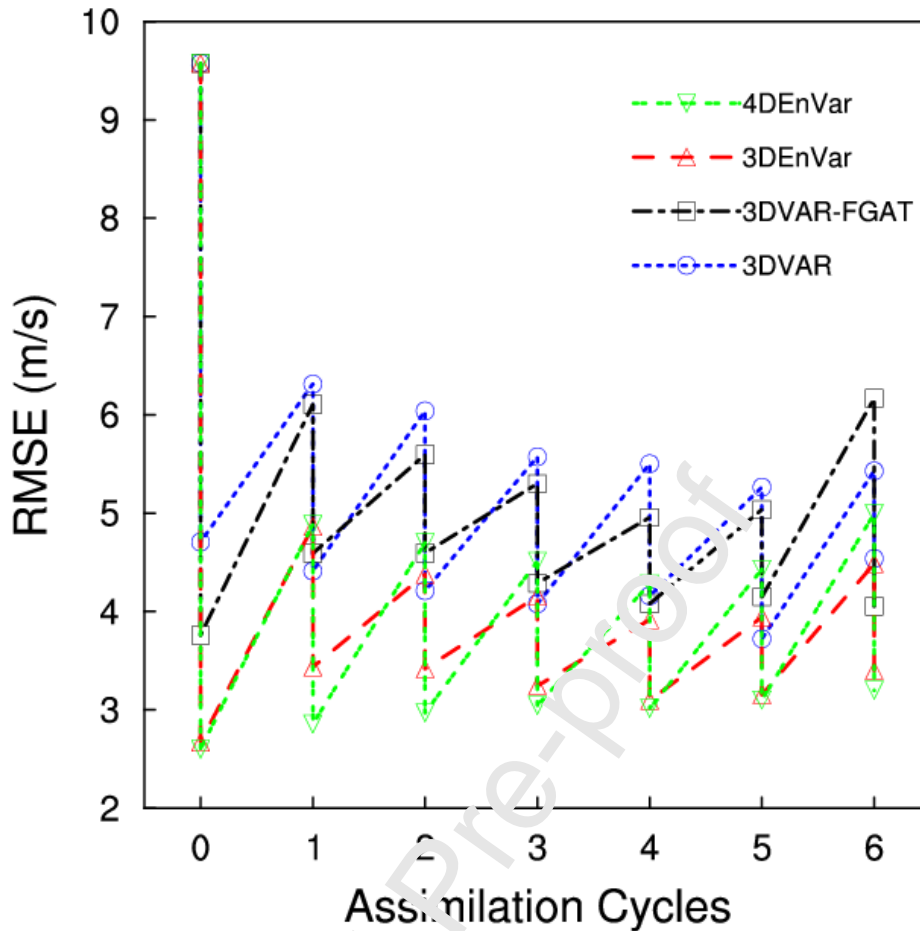


Fig. 10. The forecast and analysis (sawtooth pattern during DA cycling) for RMSE of radial velocity (m/s) a) for 3DVar, 3DVar-FGAT, 3DEnVar, and 4DEnVar from 0000 to 0300 UTC on 13 September 2008.

### 5.3 Verification for the forecasts

Fig. 11a displays the 18-h track initialized from 0000 UTC 13 September 2008 for Ike in all experiments. It is found that the track errors are relatively small for the first 3-4 hours. There is an increasing northeastward track bias from 3DVar. For the track error in Fig. 11b, in the first 12-h, 4DEnVar is better than both 3DEnVar and 3DVar-FGAT, while 3DVar produced largest track error. In the later hours, there is no consistent improvement from 3DEnVar and 3DVar-FGAT compared to 3DVar, while the track error still favors 4DEnVar. The 18-h evolution of the intensity

verification for the MSLP and the maximum surface wind (MSW) are shown in Fig. 11c and d. 4DEnVar captures the pressure closest to the best track especially after 6-h forecast. The limited improvement from 3DVar-FGAT and 3DEnVar might have been constrained by the lack of the BEC description spatially and temporally.

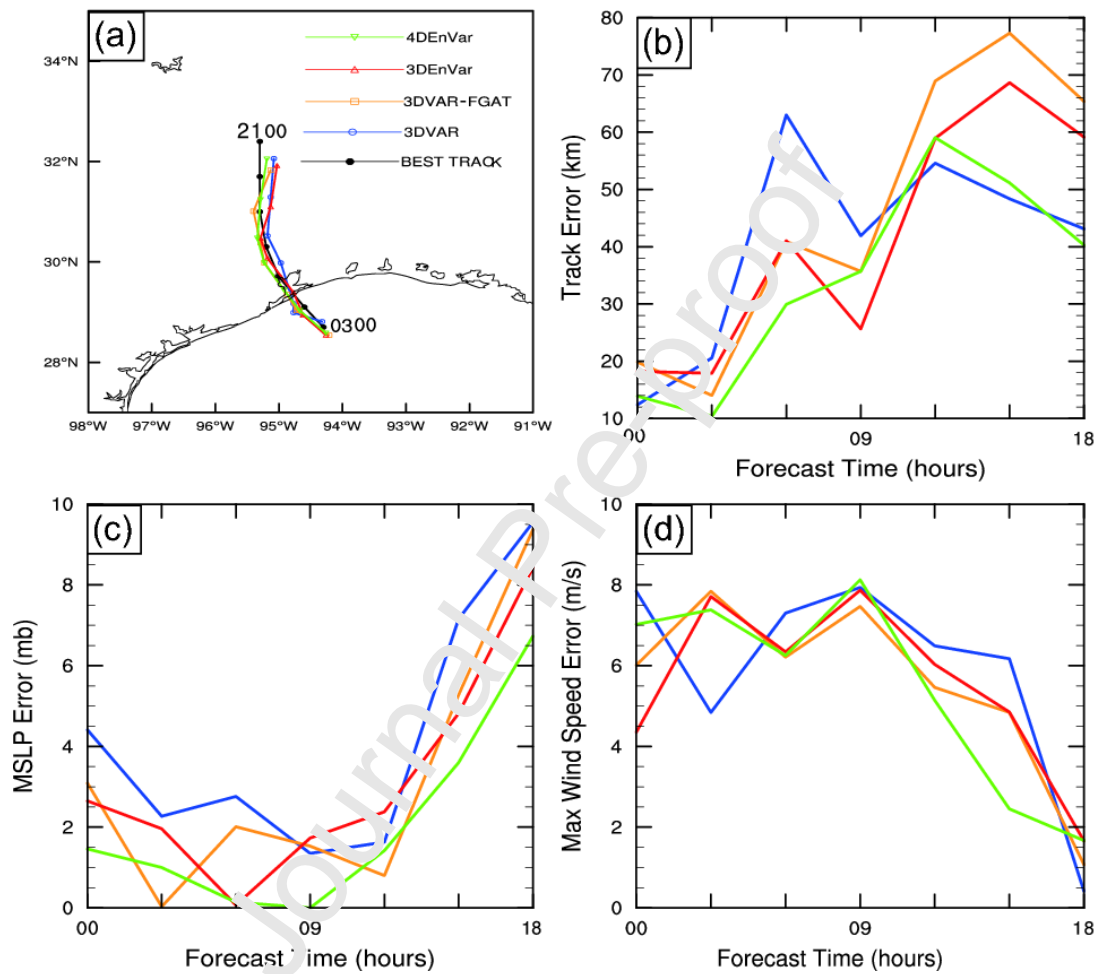


Fig. 11. The 18 h predicted (a) tracks, (b) track errors, (c) minimum surface level pressure (hPa), and (d) maximum surface wind speed (m/s) of hurricane Ike from 0300 UTC to 2100 UTC September 13, 2008.

Improving the skills of rainfall forecasts for TCs are vital for warnings of inland floods. The equitable threat scores (ETSs) are illustrated for different precipitation thresholds following the metrics in Schaefer 1990 (Fig. 12). ETSs are calculated based on the 6 h accumulated precipitation from the three experiments against the observations from the NCEP Stage-IV precipitation data from 0600 UTC to 1200

UTC September 13, 2008. Generally, there are higher ETS scores in 4DEnVar than those of other experiments, which might result from the improved track, intensity, and structure forecasts of hurricane Ike. For larger thresholds, the improvements from 4DEnVar is even significant. 3DVar obviously shows little skill in heavy rain precipitation for thresholds above 10 mm. It is found that ETSs from 3DEnVar are slightly lower than those in 4DEnVar.

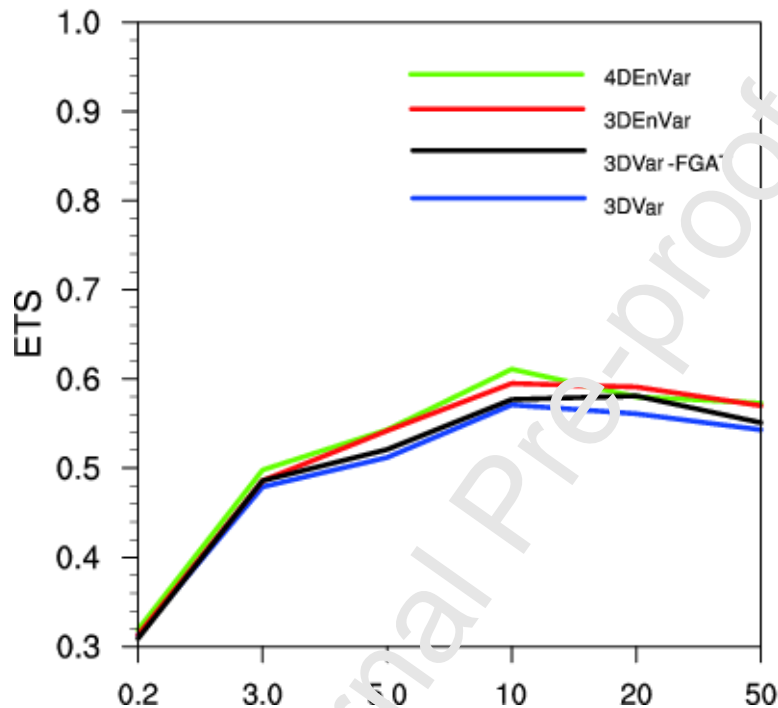


Fig. 12. Equitable threat score of 5 h accumulated precipitation verified against NCEP Stage-IV, for 3DVar, 3DVar-FGAT, 3DEnVar, and 4DEnVar from 0600 UTC to 1200 UTC September 13, 2008 for different threshold (mm).

## 6. Conclusions and future plans

The four dimensional ensemble-variation data assimilation (4DEnVar) is the method that considers the flow dependent BEC temporally and spatially. The released version of hybrid-4DEnVar system of the WRF model is investigated in terms of the radar radial velocity ( $V_r$ ) assimilation for the analysis and prediction of hurricane Ike (2008). This study serves as the initial work of examining the impact of assimilation radar  $V_r$  observations on the analyses and forecasts for a hurricane case using the WRF hybrid-4DEnVar method. The hybrid-4DEnVar is coupled with ETKF by

updating the ensemble mean by the hybrid scheme and the ensemble perturbations are updated by the ETKF in this study.

Firstly, single observation tests for typical jet case and TC case are conducted before the real case. It is found that ensemble with more samples is able to better capture the error of the day. There are heterogenous structures in the analysis increment at the beginning of the window, with the “errors of the day” captured by the ensemble covariance. It is found that the analysis increment moves downstream by the end of the assimilation window. Also note that the linear propagation represented by the 4DEnVar method is close to the full nonlinear model integration.

For the real case, positive temperature increments with spiral structures are found in the core area of Ike from 4DEnVar experiment, indicating a more realistic thermal structure of hurricane Ike, leading to improved track and intensity forecasts. 3DEnVar and 3DVar-FGAT are limited due to by the lack of the BEC description spatially and temporally. 3DVar experiment produces much smoother and weaker increments with cold temperature increments at the hurricane vortex center at lower levels.

Preliminary results in this study are encouraging, and in the future, it is important to have a systematic evaluation of the impact choosing appropriate assimilation window length and number of time slots when assimilating radar Vr data in real atmospheric model. Further work is also planned to for expanding the more observation types and other sever weather systems. Further studies with more TCs that are in different regions and at various stages of development are needed to better understand the impacts of hybrid-4DEnVar assimilation method and to obtain statistically robust results. Our effort in this study represents a step in that direction.

**Acknowledgements** This research was primarily supported by the National Key R&D Program of China (2018YFC1506404, 2018YFC1506603), the National Natural Science Foundation of China (G41805070, G41805016), the Natural Science Foundation of Jiangsu Province (BK20160954, BK20170940), the Joint Open Project of KLME & CIC-FEMD, NUIST (KLME201807, KLME201808), the Beijing Funding from Jiangsu Research Institute of Meteorological Science (BJG201604), and the Priority Academic Program Development of Jiangsu Higher Education

Institutions (PAPD).

Journal Pre-proof

- Andrew, C. L., Bowler, N. E., Clayton, A. M., Stephen R. P., 2014. Comparison of Hybrid-4DVar and Hybrid-4DVar Data Assimilation Methods for Global NWP. *Mon. Wea. Rev.* 143,212–229.
- Barker, D., Coauthors., 2012. The Weather Research and Forecasting Model's community variational/ensemble data assimilation system: WRFDA. *Bull. Amer. Meteor. Soc.* 93, 831–843.
- Barret B., et. al., 2008. Transport pathways of CO in the African upper troposphere during the monsoon season: a study based upon the assimilation of spaceborne observations. *Atmospheric Chemistry and Physics*, 8, 3231-3246.
- Bishop, C. H., Etherton, B. J., Majumdar, S. J., 2001. Adaptive sampling with the ensemble transform Kalman filter. Part I: Theoretical aspects. *Mon. Wea. Rev.* 129, 420–436.
- Buehner, M., Houtekamer, P. L., Charette, C., Mitchell, H. L., He, B., 2010a. Intercomparison of variational data assimilation and the ensemble Kalman filter for global deterministic NWP. Part I: Description and single-observation experiments. *Mon. Wea. Rev.* 138, 1550–1566.
- Buehner, M., Houtekamer, P. L., Charette, C., Mitchell, H. L., He, B., 2010b. Intercomparison of variational data assimilation and the ensemble Kalman filter for global deterministic NWP. Part II: One-month experiments with real observations. *Mon. Wea. Rev.* 138, 1567–1586.
- Buehner, M., Morneau, J., Charette, C., 2013. Four-dimensional ensemble-variational data assimilation for global deterministic weather prediction. *Nonlinear Processes Geophys.* 20, 669–682.
- Buehner, M., 2005. Ensemble-derived stationary and flow-dependent background-error covariances: Evaluation in a quasi-operational NWP setting. *Q. J. R. Meteor. Soc.* 131, 1013–1043.
- Desroziers, G., Camino, J.-T. and Berre, L., 2014. 4DVar: Link with 4D state formulation of variational assimilation and different possible implementations. *Q. J. R. Meteor. Soc.* 140, 2097–2110.
- Dowell, D. C., Zhang, F., Wicker, L. J., Snyder, C., Crook, N. A. 2004. Wind and temperature retrievals in the 17 May 1981 Arcadia, Oklahoma, supercell: Ensemble Kalman filter experiments. *Mon. Wea. Rev.* 132, 1982–2005.
- Dudhia, J., 1989. Numerical study of convection observed during the winter monsoon experiment using a mesoscale, two-dimensional model. *J. Atmos. Sci.* 46, 3077–3107.

- Evensen, G., 1994. Sequential data assimilation with a nonlinear quasi-geostrophic model using Monte Carlo methods to forecast error statistics. *J. Geophys. Res.* 99, 10143–10162.
- Fairbairn, D., S. R. Pring, A. C. Lorenc, and I. Roulstone, 2014. A comparison of 4DVar with ensemble data assimilation methods. *Quart. J. Roy. Meteor. Soc.*, 140, 281–294.
- Grell, G.A., Devenyi, D., 2002. A Generalized Approach to Parameterizing Convection Combining Ensemble and Data Assimilation Techniques. *Geophysical Research Letters*, 29, 1–4.
- Hamill, T.M., and C. Snyder, 2000. A hybrid ensemble Kalman filter–3D Variational analysis scheme. *Mon. Wea. Rev.* 128, 2905–2919.
- Hong, S.Y., Dudhi, J. S., Chen., H., 2004. A revised approach to ice microphysical processes for the bulk parameterization of clouds and precipitation. *Mon. wea. Rev.* 132, 103–120.
- Hu, X. M., Klein, P. M. Xue, M., 2013. Evaluation of the updated YSU planetary boundary layer scheme within WRF for wind resource and air quality assessments. *J. Geophys. Res.* 118, 10490-10505.
- Poterjoy, J. and F. Zhang, 2016. Comparison of Hybrid Four-Dimensional Data Assimilation Methods with and without the Tangent Linear and Adjoint Models for Predicting the Life Cycle of Hurricane Karl (2010). *Mon. Wea. Rev.*, 144, 1449–1468.
- Kleist, D. T., Ide, K. 2015a. An OSSE-based evaluation of hybrid variational–ensemble data assimilation for the NCEP GFS. Part I: System description and 3D-Hybrid results. *Mon. Wea. Rev.* 143, 433–451.
- Kleist, D. T., and K. Ide. 2015b. An OSSE-based evaluation of hybrid variational–ensemble data assimilation for the NCEP GFS. Part II: 4D-EnVar and hybrid variants. *Mon. Wea. Rev.* 143, 452–470.
- Lawless, A. S., 2010. A note on the analysis error associated with 3D-FGAT. *Q. J. R. Meteor. Soc.* 136, 1094–1098.
- Li, Y., Wang, X., Xue, M., 2012. Assimilation of radar radial velocity data with the WRF hybrid ensemble–3DVAR hybrid system for the prediction of Hurricane Ike (2008). *Mon. Wea. Rev.* 140,3507–3524.
- Liu, C., Xiao, Q., Wang, B., 2008. An ensemble-based four-dimensional variational data assimilation scheme. Part I: Technical formulation and preliminary test. *Mon. Wea. Rev.* 136,

3363–3373.

- Liu, C., Xiao, Q., Wang, B., 2009. An ensemble-based four-dimensional variational data assimilation scheme. Part II: Observing system simulation experiments with Advanced Research WRF (ARW). *Mon. Wea. Rev.* 137, 1687–1704.
- Liu, C., Xiao, Q., 2013. An ensemble-based four-dimensional variational data assimilation scheme. Part III: Antarctic applications with Advanced Research WRF using real data. *Mon. Wea. Rev.* 141, 2721–2739.
- Lorenc, A. C., 2003. The potential of the ensemble Kalman filter for NWP—A comparison with 4D-VAR. *Quart. J. Roy. Meteor. Soc.* 129, 3183–3203.
- Lorenc, A. C., N. E. Bowler, A. M. Clayton, S. R. Pring, and D. Fairbairn, 2015. Comparison of hybrid-4D-EnVar and hybrid-4DVar data assimilation methods for global NWP. *Mon. Wea. Rev.* 143, 212–229.
- Lu, X., X. Wang, M. Tong, and V. Tallapragada. 2017. GSI-Based, Continuously Cycled, Dual-Resolution Hybrid Ensemble–Variational Data Assimilation System for HWRF: System Description and Experiments with Edouard (2014). *Mon. Wea. Rev.* 145, 4877–4898.
- Pan, Y., K. Zhu, M. Xue, X. Wang, M. Mu, S. G. Benjamin, S. S. Weygandt, and J. S. Whitaker (2014), A regional GSI-based EnKF-variational hybrid data assimilation system for the Rapid Refresh configuration: Results with a single, reduced resolution, *Mon. Weather Rev.*, 142, 3756–3780.
- Mlawer, E. J., Taubman, S. J., Brown, P. D., Iacono, M. J., Clough, S. A., 1997. Radiative transfer for inhomogeneous atmospheres: RRTM, a validated correlated-k model for the longwave. *J. Geophys. Res.* 102, 16663–16682.
- Noh, Y., Cheon, W. G., Hong, S. Y., Raasch, S., 2003. Improvement of the K-profile model for the planetary boundary layer based on large eddy simulation data. *Boundary-Layer Meteorology.* 107, 401–427.
- Qiu, C., Zhang, L., Shao, A., 2007. An explicit four-dimensional variational data assimilation method. *Sci. China Ser. D: Earth Sci.* 50, 1232–1240.
- Rabier, F., Thépaut, J.-N., Courtier, P., 1998. Extended assimilation and forecast experiments with a four-dimensional variational assimilation system. *Q. J. R. Meteor. Soc.* 124, 1861–1887.

- Schaefer J. T. 1990. The critical success index as an indicator of warning skill. *Weather Forecasting* 5: 570–575.
- Schwartz, C. S., Z. Q. Liu., X. Y. Huang., 2015. Sensitivity of Limited-Area Hybrid Variational-Ensemble Analyses and Forecasts to Ensemble Perturbation Resolution. *Mon. Wea. Rev.* 143, 3454–3477.
- Shen, F., J. Z. Min., 2015. Assimilating AMSU-A Radiance Data with the WRF Hybrid En3DVAR System for Track Predictions of Typhoon Megi.,2010. *Advances in Atmospheric Sciences.* 32, 1231–1243.
- Shen, F., M. Xue., J. Min., 2017. A comparison of limited-area 3DVAR and ETKF-En3DVAR data assimilation using radar observations at convective scale for the prediction of Typhoon Saomai (2006). *Meteorol. Appl.* 24, 628–641.
- Shen F., Min, J., Xu., D., 2016. Assimilation of radar radial velocity data with the WRF Hybrid ETKF–3DVAR system for the prediction of Hurricane Ike (2008). *Atmospheric Research.* 169,127–128.
- Skamarock, W., et al., 2008. A description of the Advanced Research WRF version 3. In NCAR Tech Note NCAR/TN-475+STR, 113. NCAR.
- Sun J., Wang H., Tong W., et al., 2015. Comparison of the Impacts of Momentum Control Variables on High-Resolution Variational Data Assimilation and Precipitation Forecasting. *Mon. Wea. Rev.* 144,149–159.
- Tian, X., Z. Xie., A. Dai, 2008. An ensemble-based explicit four-dimensional variational assimilation method. *J. Geophys. Res.* 113, D21124.
- Vialard, J., A. T. Weaver., D. L. T. Anderson., P. Delecluse., 2003. Three- and four-dimensional variational assimilation with a general circulation model of the tropical Pacific Ocean. Part II: Physical validation. *Mon. Wea. Rev.* 131, 1379–1395.
- Wang, B., Coauthors., 2010. An economical approach to four dimensional variational data assimilation. *Adv. Atmos. Sci.* 27, 715–727.
- Wang, H., J. Sun, X. Zhang, X.-Y. Huang, and T. Auligné, 2013a. Radar data assimilation with WRF 4D-Var. Part I: System development and preliminary testing. *Mon. Wea. Rev.* 141, 2224–2244.

- Wang, X., 2010. Incorporating ensemble covariance in the Gridpoint Statistical Interpolation (GSI) variational minimization: A mathematical framework. *Mon. Wea. Rev.* 138, 2990–2995.
- Wang, X., T. Lei., 2014. GSI-based four-dimensional ensemble–variational (4DEnsVar) data assimilation: Formulation and single-resolution experiments with real data for the NCEP Global Forecast System. *Mon. Wea. Rev.* 142, 3303–3325.
- Wang, X., C. Snyder., T. M. Hamill., 2007. On the theoretical equivalence of differently proposed ensemble/3D-Var hybrid analysis schemes. *Mon. Wea. Rev.* 135, 222–227.
- Wang, X., D. Barker., C. Snyder., T. M. Hamill., 2008a. A hybrid ETKF-3DVAR data assimilation scheme for the WRF model. Part I: Observing system simulation experiment. *Mon. Wea. Rev.* 136, 5116–5131.
- Wang, X., D. Barker., C. Snyder., T. M. Hamill., 2008b. A Hybrid ETKF-3DVAR Data Assimilation Scheme for the WRF Model. Part II: Real Observation Experiments. *Mon. Wea. Rev.*, 136, 5132–5147.
- Wang, X., D. Parrish., D. Kleist., J. S. Whitaker., 2013b. GSI 3DVar-based ensemble–variational hybrid data assimilation for NCEP Global Forecast System: Single-resolution experiments. *Mon. Wea. Rev.* 141, 4098–4117.
- Weaver, A. T., J. Vialard., D. L. T., Anderson., 2003. Three- and four-dimensional variational assimilation with a general circulation model of the tropical Pacific Ocean. Part I: Formulation, internal diagnostics, and consistency checks. *Mon. Wea. Rev.* 131, 1360–1378.
- Yussouf, N., J. D. Gao., D. J. Stensrud., G. Q. Ge., 2013. The Impact of Mesoscale Environmental Uncertainty on the Prediction of a Tornadic Supercell Storm Using Ensemble Data Assimilation Approach. *Advances in Meteorology*.

No conflict of interest of the manuscript “Assimilation of Radar Radial Velocity Data with the WRF Hybrid 4DEnVar System for the Prediction of Hurricane Ike (2008)”

Journal Pre-proof

**Highlights:**

- The analysis increment moves downstream by the end of the assimilation window in 4DEnVar.
- The linear propagation represented by the 4DEnVar method is close to the full nonlinear model integration.
- Positive and spiral temperature increments, best track and intensity forecast are found in 4DEnVar experiment.
- 3DVar experiment produces much smoother and weaker increments at the hurricane vortex center.

Journal Pre-proof